Supplementary tables

Supplementary Table 1. Clinical and pathological features of pancreatic ductal adenocarcinoma with fluid-derived oraganoid establishment.

Patients	PDO4F1	PDO15F2	PDO17F2	PDO27F1	PDO30F1	PDO31F1	PDO32F1
Sex	F	M	M	M	M	M	F
Age	68	56	67	80	63	48	53
Diagnosis	PDAC	PDAC	PDAC	PDAC	PDAC	PDAC	PDAC
Sample	ascites	ascites	ascites	ascites	pleural effusion	ascites	ascites
KRAS	G12V	G12R	G12D	G12D	G12D	G12D	G12D
Histology	Negative for malignancy	Atypical cells, suggestive of metastatic carcinoma	Atypical cells, suspicious for metastatic carcinoma	Positive for malignancy, metastatic adenocarcinoma	Positive for malignancy, metastatic adenocarcinoma	Atypical cells	Atypical cells
Location	Head	Tail	Head	Body	Head	Body and tail	Body
Duration of response	98	90	202	78	59	250	188
Responder/Nonresponder	Nonresponder	Nonresponder	Responder	Nonresponder	Nonresponder	Responder	Responder
Prior chemotherapy history	Gemcitabine + nab-paclitaxel	Gemcitabine + nab-paclitaxel	Gemcitabine + nab-paclitaxel	Gemcitabine + nab-paclitaxel	Gemcitabine + nab-paclitaxel	Gemcitabine + nab-paclitaxel	FOLFIRINOX

Supplementary Table 2. Clinical, patological, and morphological characteristics of serially metached pancreatic ductal adenocarcinoma patient samples used for fluid-derived organoid establishment and growth rate analysis

Patients	PDO15F1	PDO15F2	PDO17F1	PDO17F2
Sex	M	M	M	M
Age	56	56	67	67
Diagnosis	PDAC	PDAC	PDAC	PDAC
Sample	Pleural effusion	ascites	pleural effusion	ascites
KRAS	G12R	G12R	G12D	G12D
Histology	Atypical cells, suggestive of metastatic carcinoma	Atypical cells, suggestive of metastatic carcinoma	N/A	Atypical cells, suspicious for metastatic carcinoma
Location	Tail	Tail	Head	Head
Morphology	cystic	cystic	Compact and cystic	Compact and cystic
Growth rate (Time to reach 3 passages, days)	61	56	112	92

Supplementary Table 3. Top 30 differentially expressed genes between fluid-derived organoids from responder and non-responders, ranked by fold change.

Gene	Regulation
CALB2	Upregulated
CEMIP	Upregulated
AZGP1	Upregulated
PCK1	Upregulated
CXCL17	Upregulated
LY6D	Upregulated
RPL10P9	Upregulated
SERPINA3	Upregulated
PSCA	Upregulated
CAPN6	Upregulated
AQP1	Upregulated
TFF2	Upregulated
FGF19	Upregulated
TMEM213	Upregulated
VSIG1	Upregulated
ECM1	Upregulated
GNE	Upregulated
EYA2	Upregulated
PGC	Upregulated
COL28A1	Downregulated
MUCL3	Downregulated
SLC2A3	Downregulated
KRT17	Downregulated
CXCL1	Downregulated
CFH	Downregulated
C3	Downregulated
CFAP157	Downregulated
LOXL4	Downregulated
SLC34A2	Downregulated
MAB21L4	Downregulated

Supplementary Figures

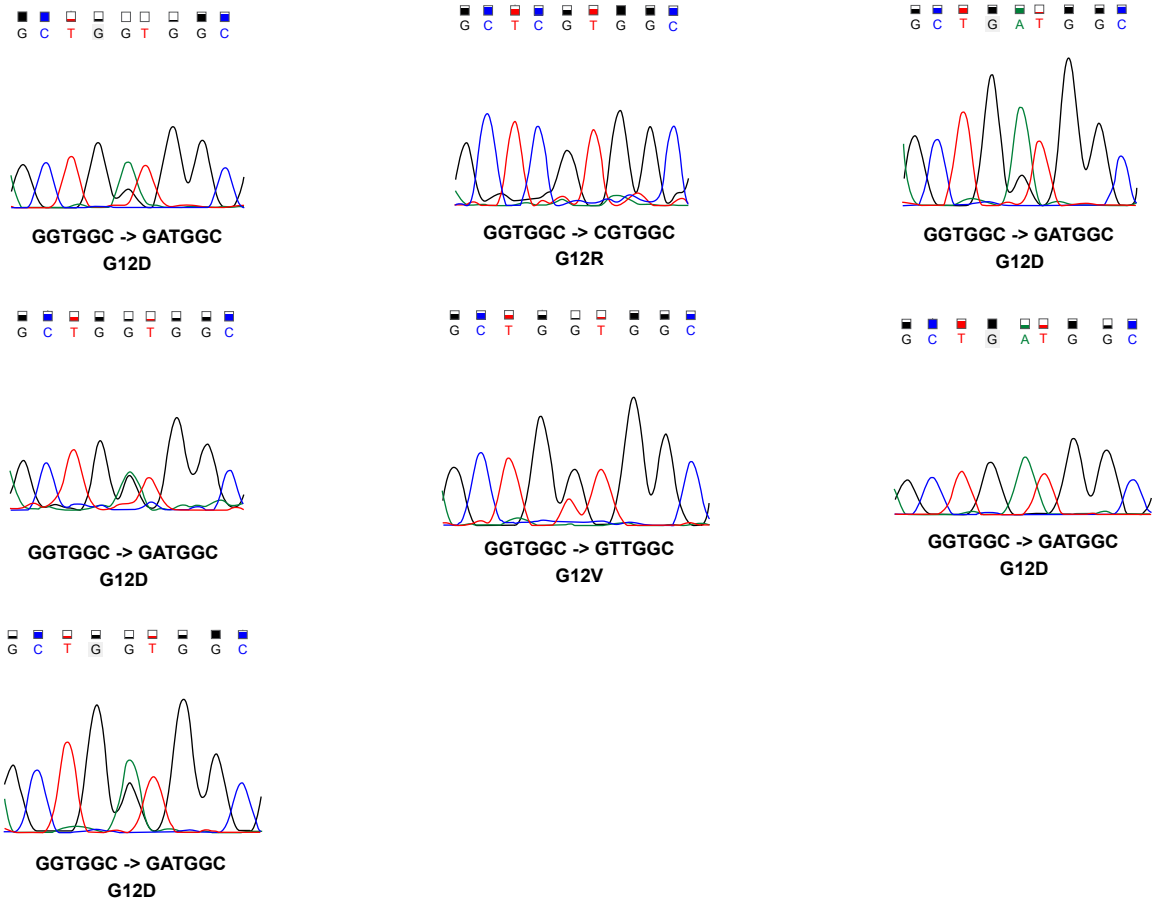

Supplementary Figure 1. *KRAS* codon 12 mutations identified in fluid-derived pancreatic cancer organoids. Sanger sequencing chromatograms demonstrating representative *KRAS* codon 12 mutations, including G12D (GGT>GAT), G12V (GGT>GTT), and G12R (GGT>CGT), in organoids derived from malignant ascites and pleural effusion of patients with pancreatic cancer. The nucleotide substitutions and corresponding amino acid changes are shown below each chromatogram.

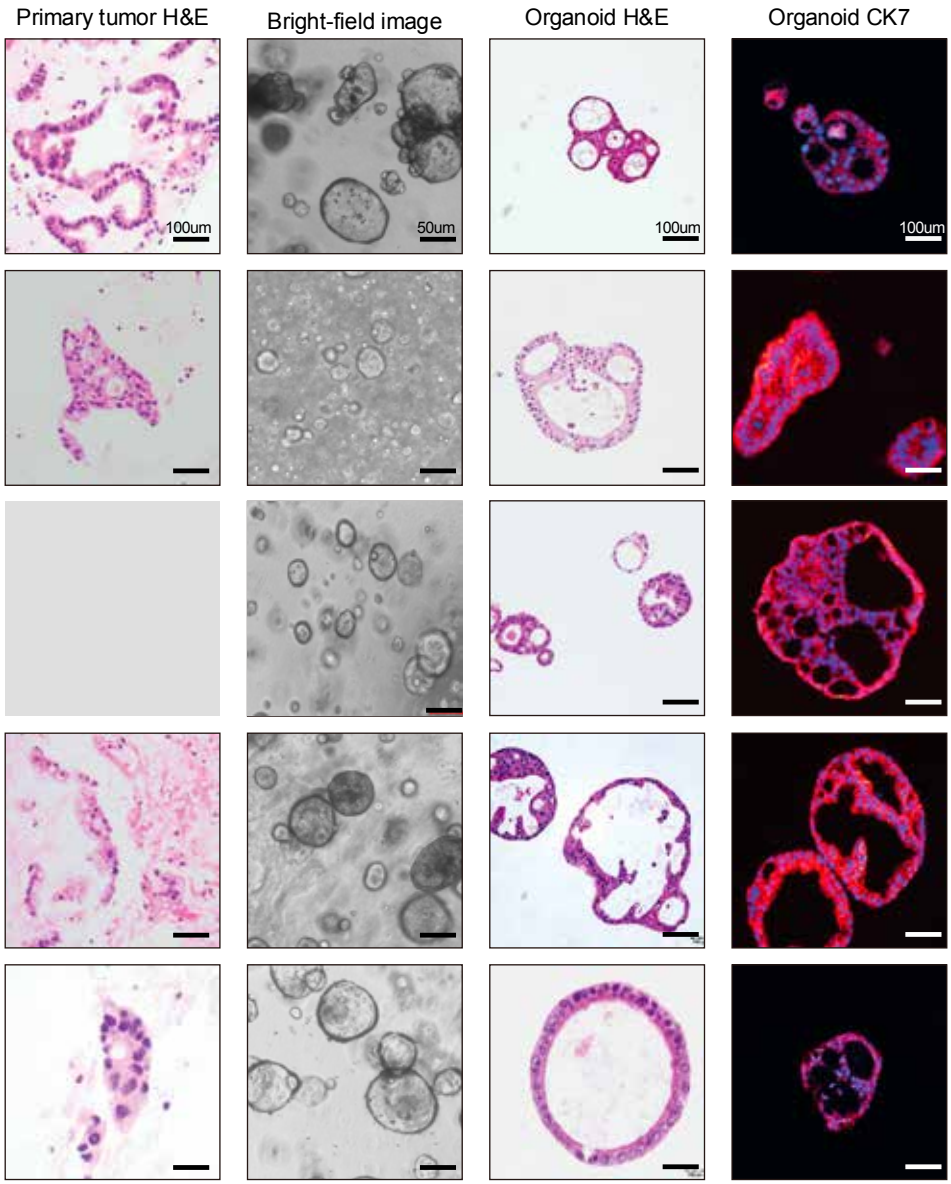

Supplementary Figure 2. Morphological comparison between primary tumor and fluid-derived organoids. Representative images of primary tumor tissue (H&E), bright-field images of organoids, and corresponding organoid sections stained with H&E and CK7 immunofluorescence.

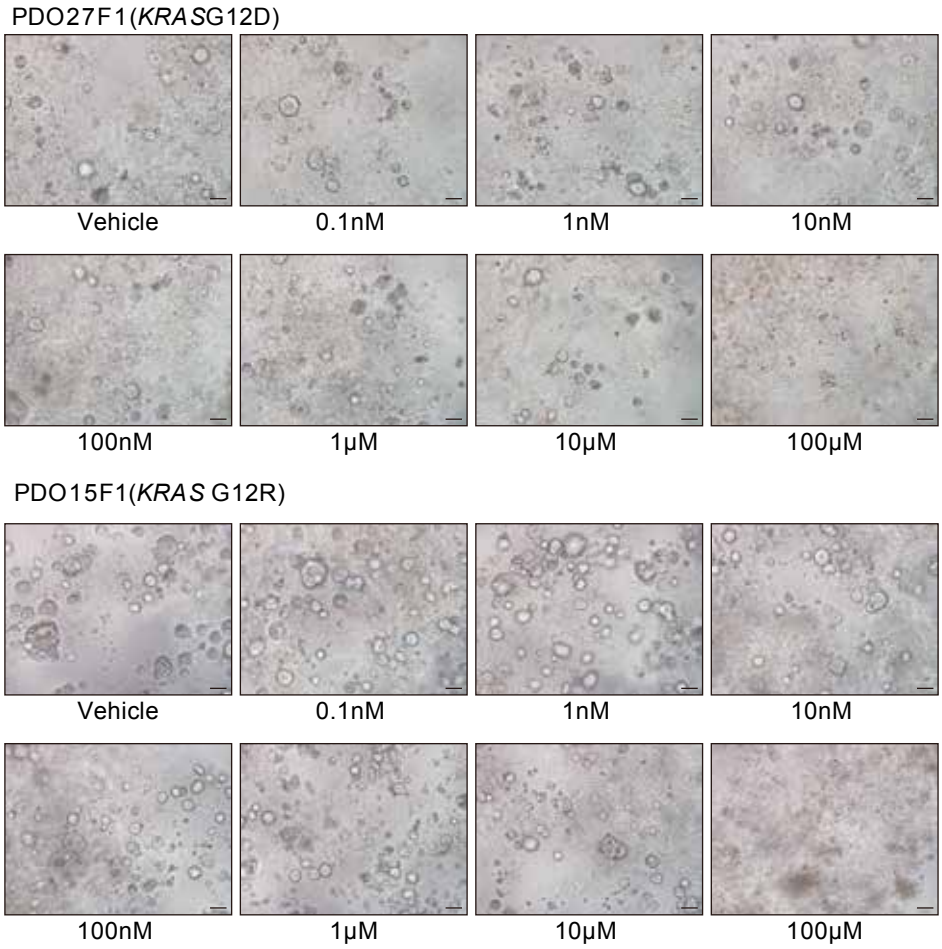

Supplementary Figure 3. Effects of MRTX1133 on fluid-derived organoids with *KRAS* G12D (PDO27F1) and G12R (PDO15F1) mutations. Bright-field images of organoids treated with increasing concentrations of the *KRAS* G12D inhibitor MRTX1133 for 72 h. PDO27F1 and PDO15F1 organoids were exposed to vehicle control or MRTX1133 at concentrations ranging from 0.1 nM to 100 μM. PDO27F1 (*KRAS* G12D) showed dose-dependent growth suppression, whereas PDO15F1 (*KRAS* G12R) showed a limited response, indicating mutation-specific sensitivity to MRTX1133. Scale bar: 50 μm

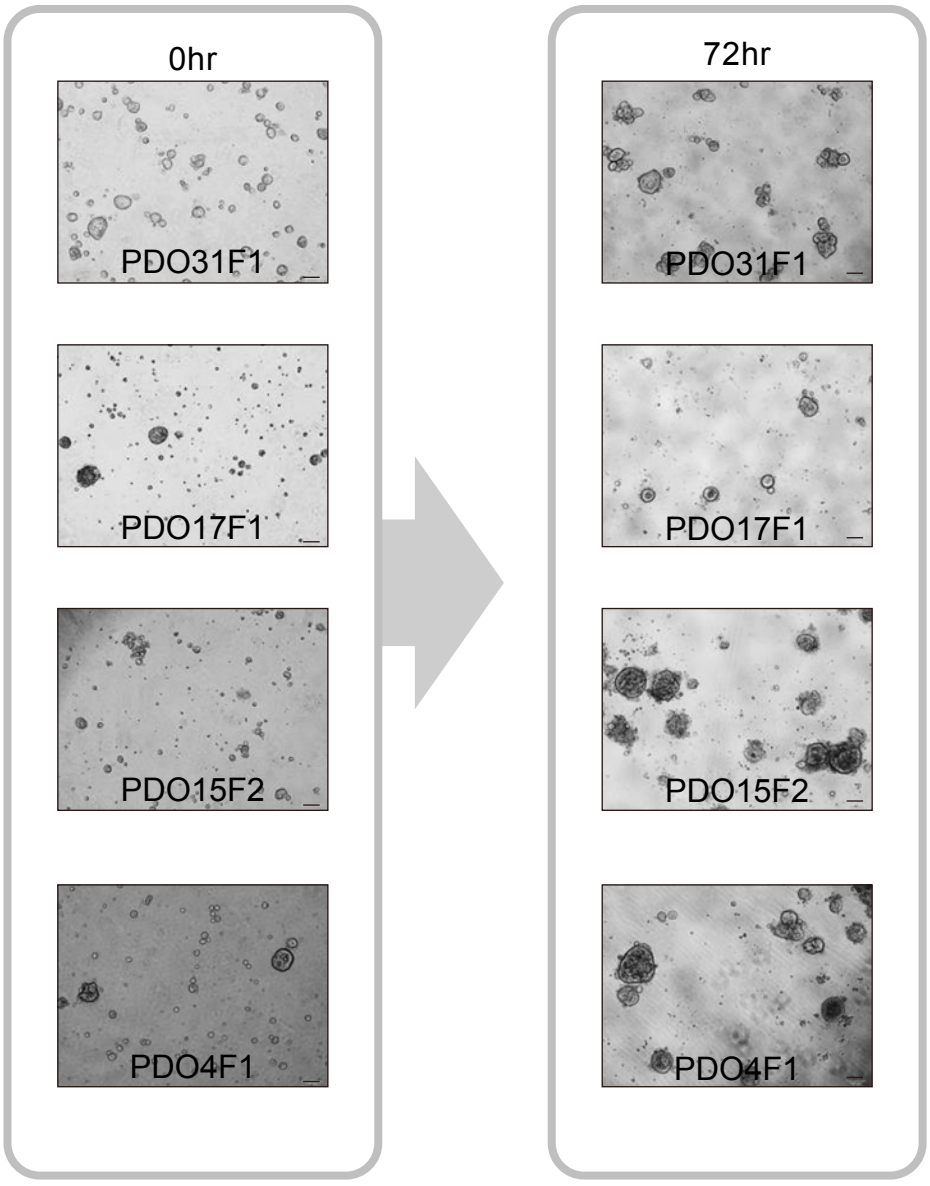

Supplementary Figure 4. Bright-field images showing organoid growth over 72 h in samples with favorable or unfavorable drug response. Representative bright-field images of FDO at 0 and 72 h. PDO31F1 and PDO17F1 were from patients with a favorable treatment response, while PDO15F2, PDO36F1, and PDO4F1 were from patients with an unfavorable response. Scale bar: 50 μm.

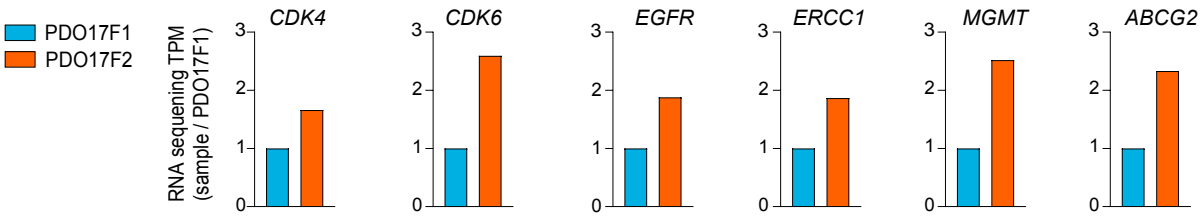

Supplementary Figure 5. Comparison of RNA sequencing-derived TPM values between PDO17F1 and PDO17F2. RNA sequencing–derived TPM values for *CDK4*, *CDK6*, *EGFR*, *ERCC1*, *MGMT*, and *ABCG2* were compared between patient-derived pancreatic cancer organoids PDO17F1 and PDO17F2. Bars represent TPM values for each gene in the indicated organoid lines.

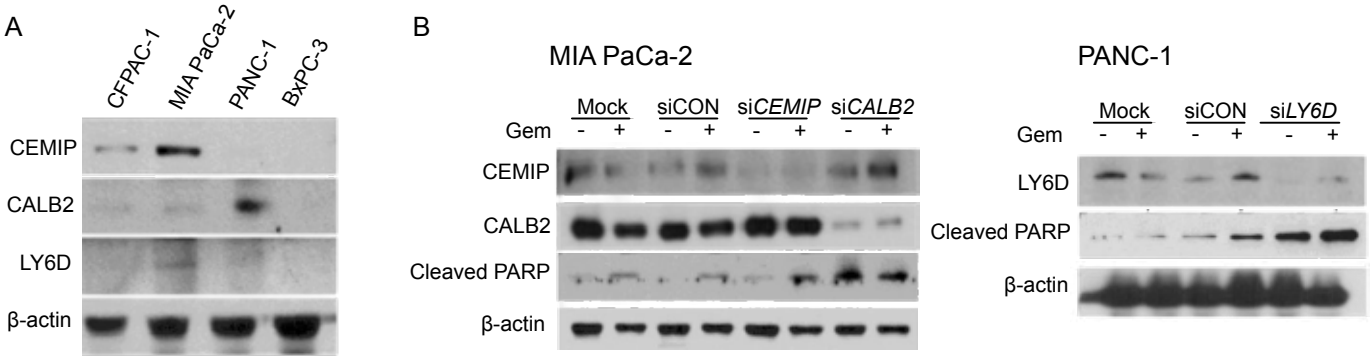

Supplementary Figure 6. Expression of CEMIP, CALB2, and LY6D in pancreatic cancer cell lines and their roles in gemcitabine sensitivity. (A) Western blotting analysis of CEMIP, LY6D, and CALB2 protein expression in four pancreatic cancer cell lines. β-Actin was used as a loading control. (B) Knockdown of *CEMIP*, *CALB2*, or *LY6D* enhanced gemcitabine-induced apoptosis. Cells were transfected with control siRNA or siRNAs targeting *CEMIP*, *CALB2*, or LY6D for 24 h, followed by gemcitabine treatment for 72 h. Apoptosis was assessed through the detection of cleaved PARP. β-Actin was used as a loading control.

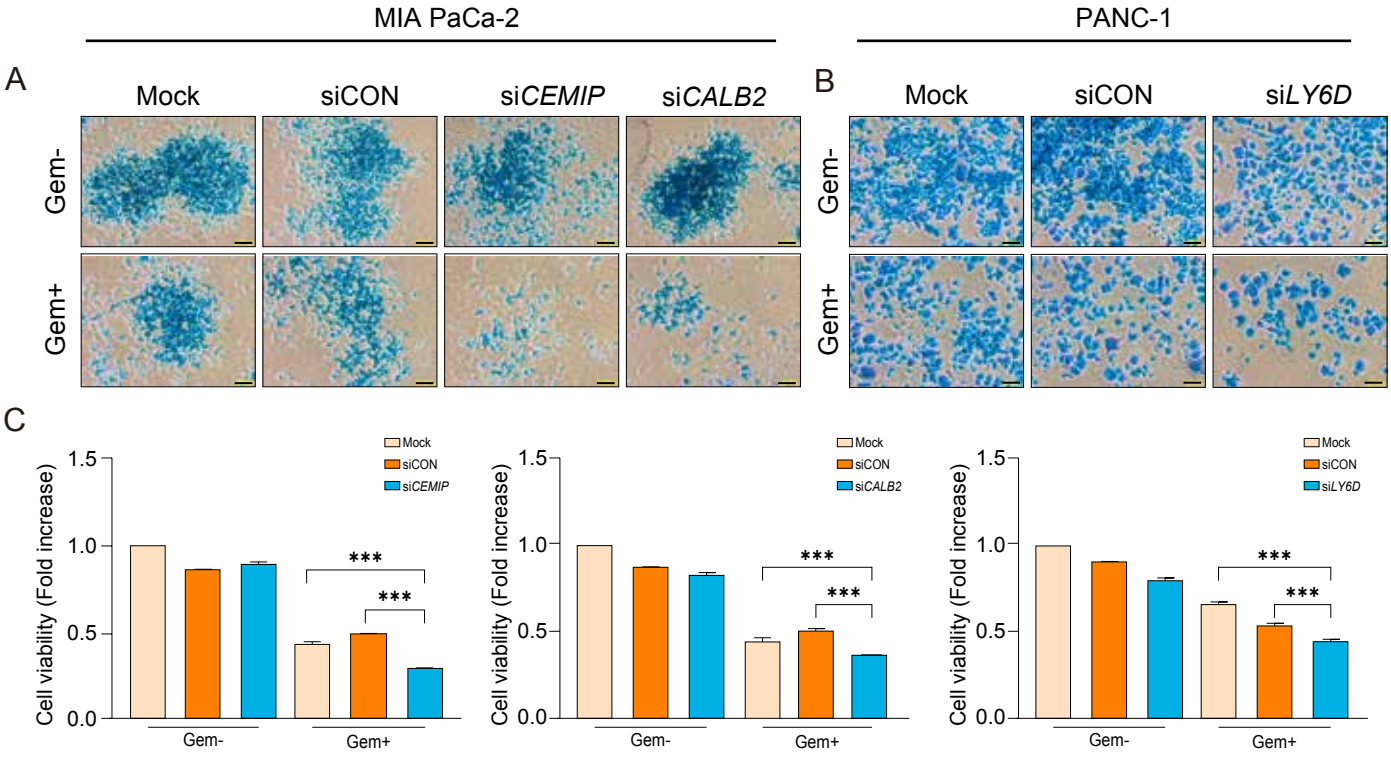

Supplementary Figure 7. CEMIP, CALB and LY6D suppress gemcitabine-induced apoptosis in pancreatic cancer cell lines. MIA PaCA-2 and PANC1 cells are transfected with control or siRNAs targeting *CEMIP*, *CALB2* or *LY6D* and treated with gemcitabine for 72 h. (A, B) Representative images of colony formation assays. (C) Quantification of colony formation in control and knockdown groups after gemcitabine treatment.

A

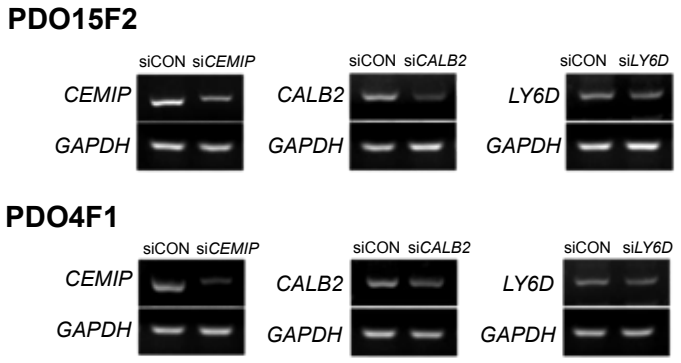

B

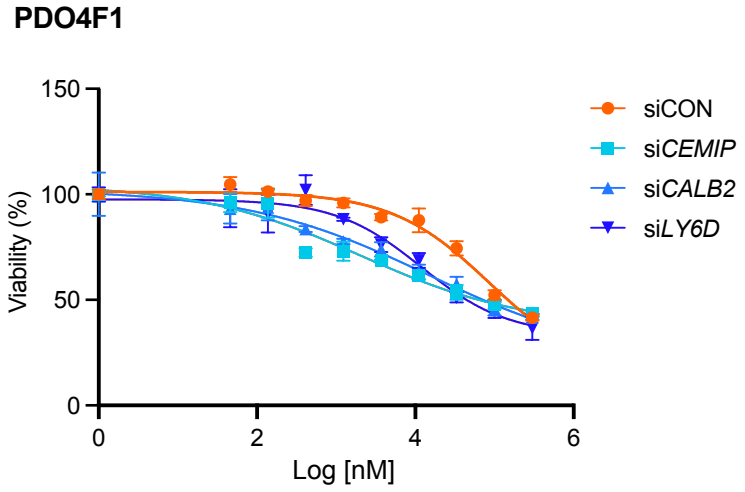

AUC (mean ± SD)	
siCON	490.0±4.5
si*CEMIP*	421.7±5.3
si*CALB2*	429.0±11.0
si*LY6D*	441.1±9.6

Supplementary Figure 8. Gene-specific knockdown enhances gemcitabine sensitivity in a non-responder pancreatic cancer organoid. (A) Patient-derived pancreatic cancer organoids (PDO15F2 and PDO4F1) were transfected with gene-specific siRNAs targeting *CEMIP*, *CALB2*, or *LY6D*, alongside a non-targeting control siRNA. Knockdown efficiency was evaluated by RT-PCR. (B) PDO4F1, previously classified as a gemcitabine non-responder, was transfected with siRNAs targeting *CEMIP*, *CALB2*, or *LY6D*, or with a non-targeting control siRNA. Following gene knockdown, organoids were treated with increasing concentrations of gemcitabine, and cell viability was measured to generate dose–response curves. The AUC was calculated to quantify drug sensitiv-

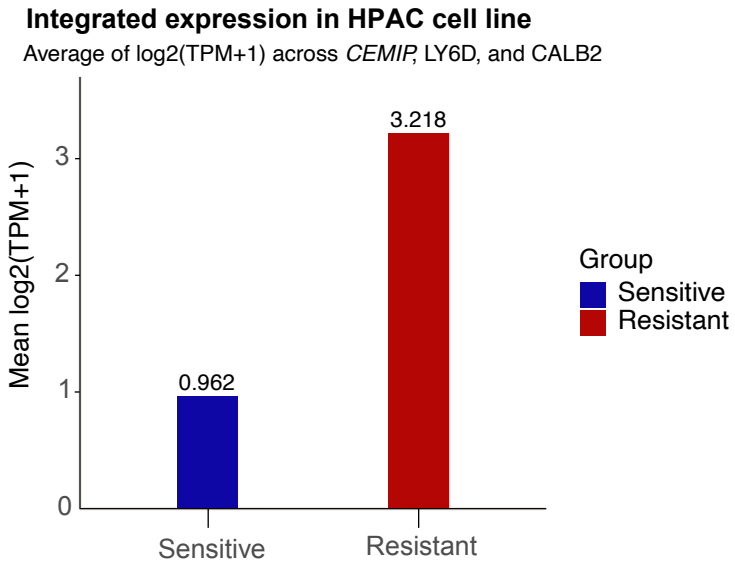

Supplementary Figure 9. Increased three-gene signature score in a gemcitabine-resistant pancreatic cancer cell line. A previously established gemcitabine-resistant HPAC cell line was analyzed. The combined three-gene signature score was compared between gemcitabine-resistant cells and their parental control cells.

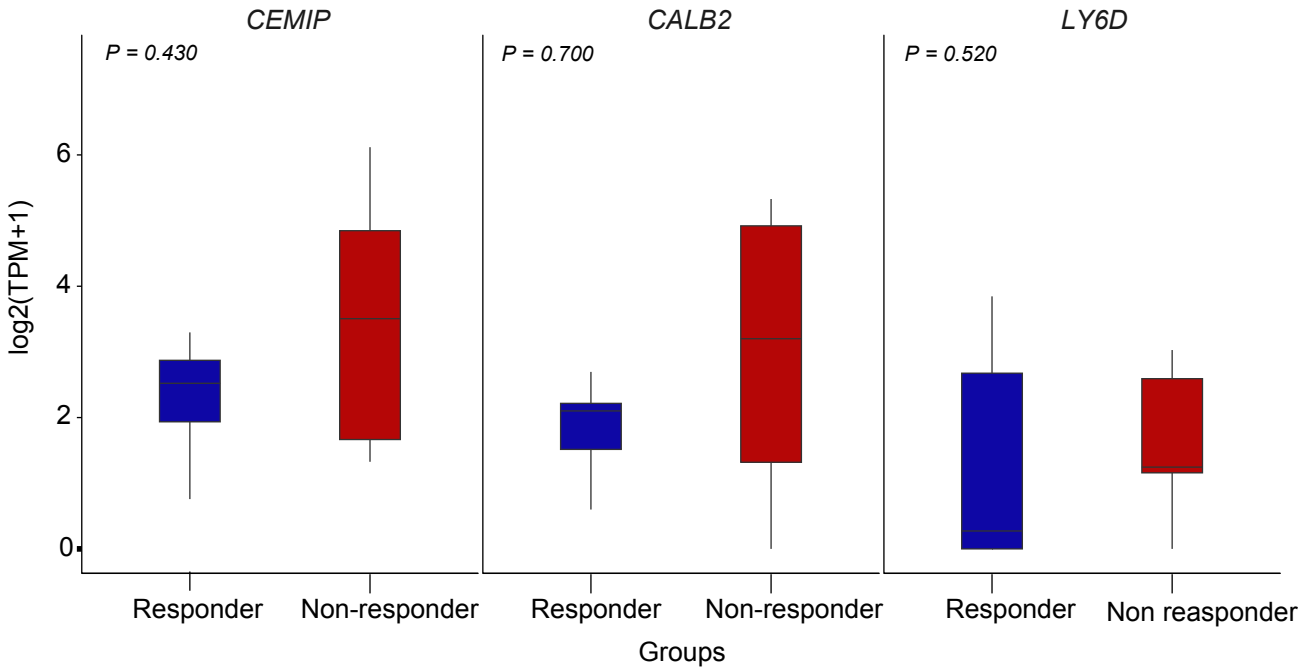

Supplementary Figure 10. Exploratory analysis of *CEMIP*, *CALB2*, and *LY6D* expression according to gemcitabine treatment response in the HMF cohort. An exploratory analysis was performed using the Hartwig Medical Foundation (HMF) dataset, focusing on patients with pancreatic cancer who received gemcitabine-based treatment (n = 35). Patients were stratified based on their first documented treatment response, with responders defined as those achieving complete response, partial response, or stable disease, and non-responders defined as those with progressive disease. The expression levels of *CEMIP*, *CALB2*, and *LY6D* were compared between the responder and non-responder groups.